



**University of  
Zurich**<sup>UZH</sup>

**Zurich Open Repository and  
Archive**

University of Zurich  
University Library  
Strickhofstrasse 39  
CH-8057 Zurich  
[www.zora.uzh.ch](http://www.zora.uzh.ch)

---

Year: 2023

---

## **Increasing Energetic Demands on Photoreceptors in Diabetes Corrects Retinal Lipid Dysmetabolism and Reduces Subsequent Microvascular Damage**

Zhang, Sheng ; Wei, Xiaochao ; Bowers, Megan ; Jessberger, Sebastian ; Golczak, Marcin ; Semenkovich, Clay F ;  
Rajagopal, Rithwick

DOI: <https://doi.org/10.1016/j.ajpath.2023.09.004>

Posted at the Zurich Open Repository and Archive, University of Zurich

ZORA URL: <https://doi.org/10.5167/uzh-253532>

Journal Article

Published Version



The following work is licensed under a Creative Commons: Attribution-NonCommercial-NoDerivatives 4.0 International (CC BY-NC-ND 4.0) License.

Originally published at:

Zhang, Sheng; Wei, Xiaochao; Bowers, Megan; Jessberger, Sebastian; Golczak, Marcin; Semenkovich, Clay F; Rajagopal, Rithwick (2023). Increasing Energetic Demands on Photoreceptors in Diabetes Corrects Retinal Lipid Dysmetabolism and Reduces Subsequent Microvascular Damage. *American Journal of Pathology*, 193(12):2144-2155.

DOI: <https://doi.org/10.1016/j.ajpath.2023.09.004>



OCULAR PATHOBIOLOGY

# Increasing Energetic Demands on Photoreceptors in Diabetes Corrects Retinal Lipid Dysmetabolism and Reduces Subsequent Microvascular Damage



Sheng Zhang,<sup>\*</sup> Xiaochao Wei,<sup>†</sup> Megan Bowers,<sup>‡</sup> Sebastian Jessberger,<sup>‡</sup> Marcin Golczak,<sup>§</sup> Clay F. Semenkovich,<sup>†¶</sup> and Rithwick Rajagopal<sup>\*</sup>

From the Departments of Ophthalmology and Visual Sciences<sup>\*</sup> and Cell Biology and Physiology<sup>¶</sup> and the Division of Endocrinology, Metabolism, and Lipid Research,<sup>†</sup> Washington University School of Medicine, St. Louis, Missouri; the Faculties of Medicine and Science,<sup>‡</sup> Laboratory of Neural Plasticity, Brain Research Institute, University of Zurich, Zurich, Switzerland; and the Department of Pharmacology,<sup>§</sup> Case Western Reserve University School of Medicine, Cleveland, Ohio

Accepted for publication  
September 1, 2023.

Address correspondence to  
Rithwick Rajagopal, M.D.,  
Ph.D., Department of Ophthalmology and Visual Sciences,  
Washington University School of Medicine, St. Louis, MO  
63110.  
E-mail: [rajagopalr@wustl.edu](mailto:rajagopalr@wustl.edu).

Mechanisms responsible for the pathogenesis of diabetic retinal disease remain incompletely understood, but they likely involve multiple cellular targets, including photoreceptors. Evidence suggests that dysregulated *de novo* lipogenesis in photoreceptors is a critical early target of diabetes. Following on this observation, the present study aimed to determine whether two interventions shown to improve diabetic retinopathy in mice—pharmacologic visual cycle inhibition and prolonged dark adaptation—reduce photoreceptor anabolic lipid metabolism. Elevated retinal lipid biosynthetic signaling was observed in two mouse models of diabetes, with both models showing reduced retinal AMP-activated kinase (AMPK) signaling, elevated acetyl CoA carboxylase (ACC) signaling, and increased activity of fatty acid synthase, which promotes lipotoxicity in photoreceptors. Although retinal AMPK-ACC axis signaling was dependent on systemic glucose fluctuations in healthy animals, mice with diabetes lacked such regulation. Visual cycle inhibition and prolonged dark adaptation reversed abnormal retinal AMPK-ACC signaling in mice with diabetes. Although visual cycle inhibition reduced the severity of diabetic retinopathy in control mice, as assessed by retinal capillary atrophy, this intervention was ineffective in fatty acid synthase gain-of-function mice. These results suggest that early diabetic retinopathy is characterized by glucose-driven elevations in retinal lipid biosynthetic activity, and that two interventions known to increase photoreceptor glucose demands alleviate disease by reversing these signals. (*Am J Pathol* 2023, 193: 2144–2155; <https://doi.org/10.1016/j.ajpath.2023.09.004>)

The early pathogenesis of diabetic retinopathy (DR) not only involves retinal blood vessels, but also the neural elements they supply.<sup>1,2</sup> In fact, compelling evidence suggests that pathology in the neural compartment of the retina—and within photoreceptors, specifically—initiates the steps that eventually cause the classic microvascular stigmata of DR.<sup>3</sup> First, electroretinography in patients with diabetes but no signs of retinopathy shows abnormal responses that localize to photoreceptors.<sup>4–6</sup> Second, patients with inactivating mutations in components of the visual transduction pathway are relatively protected from DR.<sup>7–9</sup> Third, in the Medalist

trial, a multimodal cross-sectional study of patients with >50 years' exposure to diabetes, reduced DR severity was linked to increased levels of retinol-binding protein-3 (alias

Supported by the NIH EY034172 (R.R.), EY023948 (M.G.), and P30 EY002687 (Washington University School of Medicine Department of Ophthalmology and Visual Sciences); Research to Prevent Blindness (New York, NY) unrestricted award (Washington University School of Medicine Department of Ophthalmology and Visual Sciences); the Horncrest Foundation (St. Louis, MO) unrestricted award; and Washington University Diabetes Research Center DK020579.

interphotoreceptor retinoid-binding protein), a photoreceptor protein product.<sup>10</sup>

Damaging reactive oxygen species, which promote DR development, are predominantly a by-product of photoreceptor metabolic activity.<sup>11–13</sup> Moreover, photoreceptor metabolic demands per unit of tissue mass are among the highest in the body.<sup>14</sup> These demands are largely driven by correction of the dark current, wherein ATP-dependent cation channels facilitate efflux of sodium and calcium driven intracellularly by cyclic nucleotide-gated channels that are open in the absence of light.<sup>15</sup> Such observations led to the development of a popular hypothesis that preventing dark adaptation would mitigate DR by lessening ATP requirements and, therefore, by assumption, vascular demands.<sup>16</sup> However, a phase 3 clinical trial to test this hypothesis failed in meeting its primary outcome.<sup>17</sup> Similarly, treatment of diabetic mice with a visual cycle antagonist, which prevents light-activated transduction, does not worsen DR but rather improves it.<sup>18</sup>

Therefore, mechanisms accounting for photoreceptor roles in DR and the effects of dark adaptation and visual cycle inhibition require clarification. In experimental DR, targeted genetic manipulation of photoreceptor metabolism can increase or decrease the severity of experimental DR, depending on the nature of the manipulation.<sup>19</sup> Increasing the anabolic drive of rod photoreceptors increases susceptibility to DR, whereas reducing this drive prevents the onset of DR. In streptozotocin (STZ)-induced diabetes or in *db/db* mice with spontaneous diabetes, 2 months of light deprivation reduces the severity of DR.<sup>20</sup> Similarly, in the STZ model, treatment with the visual cycle inhibitor, retinylamine, lessens capillary atrophy and reactive oxygen species formation, compared with vehicle-treated controls.<sup>18</sup>

Taking these observations together, the present study tested the hypothesis that prolonged dark adaptation or pharmacologic visual inhibition both reduce DR by increasing ATP demand and, subsequently, reducing anabolic drive, which is dependent on ATP surplus. This hypothesis predicts that in models of DR, cellular regulators of anabolic metabolism would be up-regulated and that inhibiting the visual cycle by light deprivation or pharmacologic blockade would negate these signaling processes.

## Materials and Methods

### Animals

The following mice were obtained from Jackson Laboratories (Bar Harbor, ME): C57BL/6J (stock number 000664); and leptin receptor BKS. *Cg-Dock7<sup>m+/+</sup> Lepr<sup>db/J</sup>* breeding pairs (*db/m* heterozygotes; stock number 000642). Parental *db/m* pairs were mated; and among the F<sub>1</sub> progeny, homozygous *db/db* pups (spontaneously diabetic) and heterozygous *db/m* littermates (metabolically healthy) were retained. The fatty acid synthase (FAS) R1812W transgenic line on the C57BL/6J background was used for gain-of-function

analysis, as previously described.<sup>21</sup> All animals were fed Purina (St. Louis, MO) 4043 chow (13% kcal from fat, 62% kcal from carbohydrate, and 25% kcal from protein).

### Induction of Diabetes

In some experiments, STZ was used to induce diabetes in male mice only, given the reported resistance of female C57BL/6J mice to this drug at standard doses,<sup>22</sup> although at higher doses, disease can be induced in female mice as well.<sup>23</sup> Briefly, five i.p. doses of STZ were delivered at 60 mg/kg dissolved in freshly prepared sodium citrate buffer (pH 4.5), or citrate buffer alone was delivered for controls, as previously published.<sup>19</sup> Individuals in the diabetes group were included if tail vein glucose values were >300 mg/dL.

### Housing

Animals were housed in a pathogen-free facility. For light-deprivation experiments, animals were randomly allocated (1:1) to a room with a 24-hour lights-off cycle (0 lux) or to standard housing (12 hours lights on, 1000 lux:12 hours lights off, 0 lux). Mice were given *ad libitum* access to food and water. Before sacrifice, mice were fasted for 6 hours on Aspen bedding. In some experiments, as indicated, mice were refed with chow after the fast and sacrificed either 1 or 3 hours afterward, a protocol that is comparable to previously reported refeeding time frames for both metabolic signaling assays and neuronal signaling assays.<sup>24,25</sup>

### Glucose and Insulin Administration

Dextrose (1 g/kg) dissolved in phosphate-buffered saline was delivered by i.p. injection to animals that were fasted for 6 hours. Glucose values were measured by tail blood sampling. Separate cohorts of animals were sacrificed at 10, 30, 60, and 120 minutes after injection to harvest retinas. For insulin challenge experiments, 0.75 units/kg regular insulin was provided intraperitoneally, and an otherwise identical design as described above was followed.

### Antibodies and Western Blot Analysis

After a 6-hour fast, animals were deeply anesthetized with ketamine and xylazine and then perfused with 10 mL of phosphate-buffered saline via left ventricular puncture. Two isolated retinas per animal were homogenized in a lysis buffer containing 20 mmol/L Tris (pH 8.0), 137 mmol/L NaCl, 1% Nonidet P-40, 0.25% sodium deoxycholate, 10% glycerol, 5 mmol/L NaF, and 2 mmol/L sodium orthovanadate, supplemented with a protease inhibitor cocktail. In some experiments, 5 mg of homogenized liver was lysed in the buffer described in the previous sentence. Samples were loaded at 50 µg total protein per lane. For Western blot analysis, the authors used polyclonal rabbit IgG against the  $\alpha$  subunit of AMP-activated kinase (AMPK) phosphorylated

at Thr 172 (pAMPK; catalog number 2531; Cell Signaling, Danvers, MA), rabbit IgG against acetyl CoA carboxylase (ACC) phosphorylated at Ser 79 (pACC; catalog number 3661; Cell Signaling), and rabbit IgG against  $\beta$ -actin (catalog number 4967; Cell Signaling).

### FAS Enzyme Activity

Two isolated retinas, or 5 mg of liver per animal, were homogenized in the same lysis buffer as described above for Western blot preparation. FAS activity was assessed in the lysate by providing labeled malonyl-CoA, as previously described.<sup>26</sup>

### Retinylamine Treatment

Retinylamine was synthesized and prepared as previously described.<sup>27</sup> The drug was delivered at a dose of 0.2 mg/animal dissolved in 50  $\mu$ L of dimethyl sulfoxide twice per week by i.p. injection for either 2 weeks (for electroretinography and Western blot analysis) or 3 months (for capillary morphology). Controls were dosed identically, but with 50  $\mu$ L dimethyl sulfoxide. Mice were housed in standard lighting conditions.

### Electroretinography

A UTAS BigShot System (LKC Technologies, Inc., Gaithersburg, MD) was used, according to published protocols.<sup>28</sup> In brief, mice were dark adapted overnight, anesthetized under red-light illumination, and provided a stimulus of a 10-millisecond full-field white-light flash at the indicated luminances. A contact lens electrode was used to record responses. The amplitude of the a-wave was measured from the average pretrial baseline to the most negative point of the average trace, and the b-wave amplitude was measured from that point to the highest positive point.

### Capillary Morphology

For STZ-treated animals at 8 months of age (approximately 6 months' exposure to diabetes), trypsin digests and capillary measurements were performed, as described previously.<sup>28–30</sup> Briefly, isolated retinas were fixed for 24 hours at 4°C in 4% paraformaldehyde, then treated with 3% porcine trypsin at 37°C, and then washed until only vascular skeletons remained. Tissues were flat mounted and stained with 1% periodic acid–Schiff base, with a hematoxylin counterstain. Atrophic capillaries were assessed by a masked observer (S.Z.).

### Statistical Analysis

In line graphs, data are expressed as means  $\pm$  SEM. For box-and-whisker plots, data are expressed as median, with

the box showing the interquartile range, and whiskers representing maxima and minima. For experiments with two groups in the independent variable, analyses were performed using two-tailed *t*-tests without *post hoc* correction. For experiments with more than two groups in the independent variable, one-way analysis of variance with *post hoc* correction was used when only one dependent variable was present, and two-way analysis of variance with post-tests was used when two or more dependent variables were present. All calculations were performed using GraphPad Prism 6.0 software (GraphPad Software, Boston, MA).

### Study Approval

Protocols followed the Association for Research in Vision and Ophthalmology Statement for the Use of Animals and were approved by Washington University (St. Louis, MO).

## Results

### Effects of Systemic Glucose Excursions on Retinal Lipogenic Signaling

Elevated retinal lipogenesis, driven by FAS, is an important contributor to DR.<sup>19</sup> FAS in extraocular tissues is transcriptionally regulated, but FAS message and protein levels are unchanged in the retina of mice with diabetes compared with control mice. To better understand the regulation of FAS in DR, this study interrogated post-translational control through the AMPK, which is responsive to cellular nutritional status.<sup>31</sup> AMPK acts as a primary cellular sensor of ATP availability and is activated by phosphorylation during nutrient scarcity when the AMP/ATP ratio is elevated.<sup>32</sup> In mouse, Thr 172 is the critical phosphorylation site, and upstream kinases acting at this residue include serine–threonine liver kinase B1 (LKB1) and Ca<sup>2+</sup>/calmodulin-dependent protein kinase kinase- $\beta$  (CAMKK $\beta$ ).<sup>33,34</sup> In contrast, in nutrient abundance, AMP/ATP ratios are low, and AMPK is primarily in a dephosphorylated, inactive state.

Effects of feeding and fasting on retinal AMPK phosphorylation were first assessed. In *db/db* mice, glucose levels were markedly elevated compared with the healthy *db/m* controls after a 6-hour fast and after 1 or 3 hours of refeeding (Figure 1A). As expected, fasting induced a relative hyper-phosphorylation of AMPK relative to the post-feeding periods in control mice. At 1 hour of refeeding, pAMPK levels decreased, but then increased at 3 hours of refeeding, corresponding to respective changes in blood glucose levels at each time-point (Figure 1, A–C). In *db/db* mice, however, levels of phosphorylated AMPK were lower than in *db/m* controls at baseline (fasting), and they did not show responsiveness to retinal AMPK phosphorylation with refeeding, unlike that in *db/m* counterparts (Figure 1C).

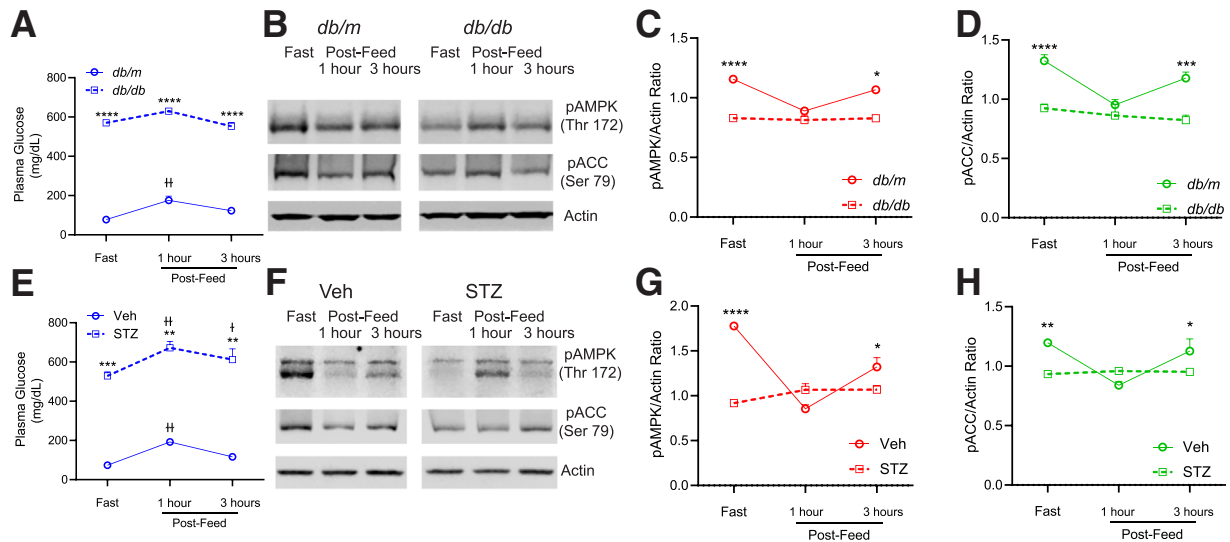


**Figure 1** Effects of diabetes on fasting and refeeding responses of retinal cellular nutrient sensors. **A–H:** The 6-month-old *db/db* mice (**A–D**) or streptozotocin (STZ)-injected mice (**E–H**) and their respective controls were analyzed for glucose excursions and retinal phosphorylated AMP-activated kinase (AMPK) and acetyl CoA carboxylase (ACC) profiles. All mice were fasted for 6 hours and then either immediately sacrificed or allowed to refeed with chow for 1 or 3 hours. **A** and **E:** Tail vein glucose values in each group were recorded. Retinal tissue from each group was analyzed for AMPK phosphorylated at Thr 172 (pAMPK) and ACC phosphorylated at Ser 79 (pACC), with all values normalized to  $\beta$ -actin levels. **B–D** and **F–H:** Representative Western blot analyses are shown (**B** and **F**), and quantified values are plotted (**C, D, G** and **H**). Data were analyzed by two-way analysis of variance with Bonferroni *post hoc* tests. Data represent means with SEM (**A, C–E, G**, and **H**). \* $P < 0.05$ , \*\* $P < 0.01$ , \*\*\* $P < 0.001$ , and \*\*\*\* $P < 0.0001$ ;  $^{\dagger}P < 0.05$ ,  $^{\ddagger}P < 0.01$ , comparing post-prandial glucose values with the fasting baseline within each group. Veh, vehicle.

In aggregate, signaling effects of pAMPK caused increased cellular ATP production via catalysis and reduced ATP use via anabolism. Lipid anabolism was further investigated in this study because this pathway is critical to maintenance of retinal health.<sup>26</sup> Control of *de novo* lipogenesis is primarily regulated by the enzyme ACC, which generates malonyl-CoA using acetyl-CoA precursors.<sup>35</sup> Newly synthesized malonyl-CoA regulates FAS, the rate-limiting enzyme in the lipogenic pathway.<sup>36</sup> In nutrient-scarce conditions, activated AMPK phosphorylates murine ACC at Ser 79, thereby inhibiting its activity.<sup>37</sup> In contrast, under nutrient-replete conditions, dephosphorylation of ACC is associated with an increase in its catalytic rate.<sup>38</sup>

In adult *db/m* mice, fasting was associated with hyperphosphorylation of ACC (inhibition) relative to 1 hour after feeding (**Figure 1, B** and **D**) with a return to near-fasting levels of phosphorylation 3 hours after feeding. Retinal ACC was hypophosphorylated in *db/db* mice relative to *db/m* controls during the fasting period and at 3 hours after refeeding. Moreover, refeeding did not result in dephosphorylation of ACC in *db/db* mice, as it did in controls (**Figure 1D**).

These experiments were repeated in STZ-injected diabetic mice. Consistent with *db/db* mice, both retinal AMPK and ACC were hypophosphorylated relative to controls during fasting and 3 hours after feeding in STZ mice (**Figure 1, E–H**). Taken together, these results suggest that a hallmark of retinal metabolic signaling in murine diabetes is inhibition of AMPK signaling, with secondary activation of the key lipogenic enzyme, ACC.

These results suggest that glucose availability drives retinal lipogenic signaling via AMPK-ACC. To discriminate between effects of glucose versus those of feeding (such as vagus nerve signaling), *i.p.* injections were used. In healthy, fasted *db/m* mice, a 1-g/kg bolus of dextrose (**Figure 2, A–D**) elevated serum glucose from a baseline of 100 mg/dL to a peak of approximately 400 mg/dL within 10 minutes, followed by a correction to near-baseline levels by 120 minutes (**Figure 2B**). In contrast, the same bolus in littermate *db/db* mice increased blood glucose from approximately 600 mg/dL to a peak of approximately 800 mg/dL at 60 minutes, with persistent elevations thereafter (**Figure 2B**). In response to an insulin bolus (0.75 units/kg) (**Figure 2, E–H**), blood glucose decreased to approximately 50 mg/dL from a fasting baseline of approximately 100 mg/dL in *db/m* mice at 10 minutes after injection, with return to baseline by 120 minutes (**Figure 2F**). In insulin-resistant *db/db* mice, blood glucose decreased only transiently from approximately 600 to 575 mg/dL at 10 minutes but quickly increased to >600 mg/dL by 30 minutes and then remained persistently elevated (**Figure 2F**).

Phosphorylation patterns of AMPK and ACC correlated with glucose excursions in *db/m* mice, with an approximately 50% reduction in pAMPK and a 40% reduction in pACC at 10 minutes after injection, and a return to near-baseline levels for both proteins at 60 minutes after injection (**Figure 2, C** and **D**). Similarly, in response to glucose lowering with insulin, retinal AMPK and ACC showed an immediate and prolonged hyperphosphorylation pattern (**Figure 2, G** and **H**). In contrast



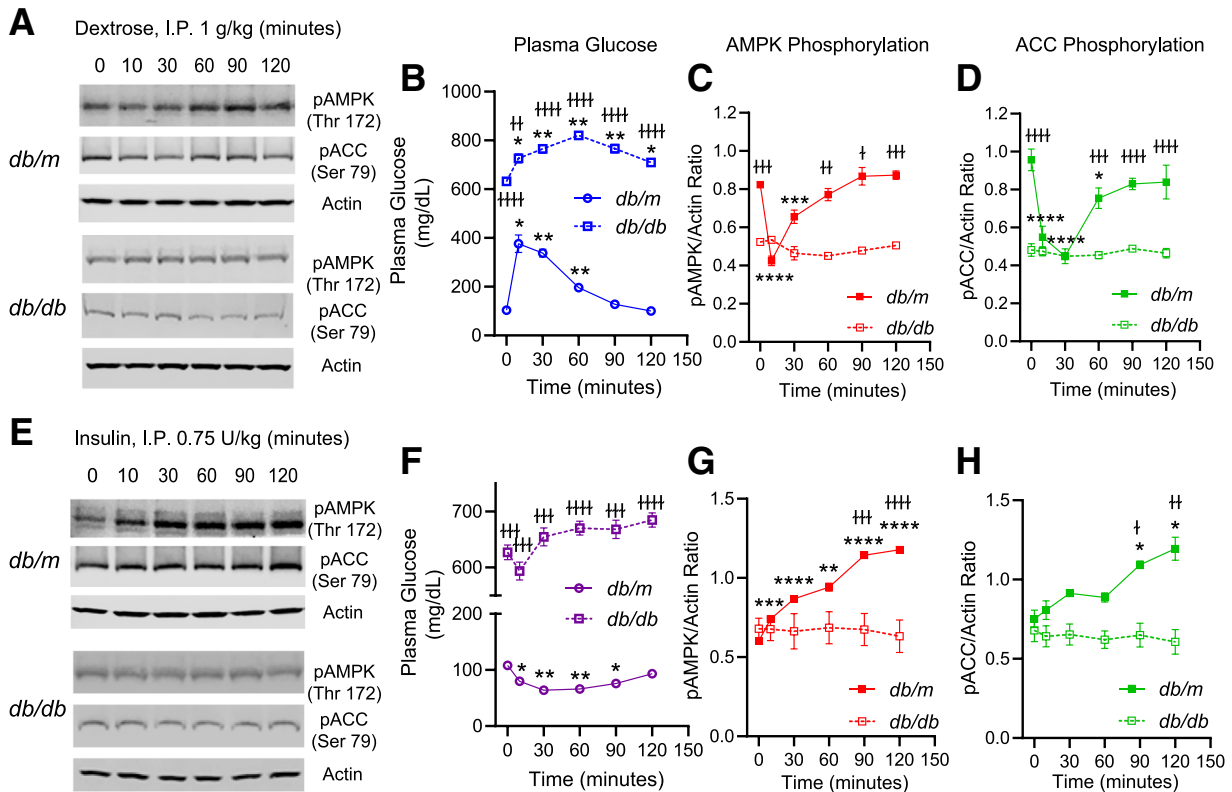


**Figure 2** Responses of retinal cellular nutrient sensors to glucose or insulin challenge in *db/db* mice. **A–H:** The 6-month-old *db/db* mice or nondiabetic *db/m* littermate controls were fasted for 6 hours and then given an i.p. dose of dextrose (**A–D**) or insulin (**E–H**). **B** and **F:** In separate cohorts, tail vein sampling was used to measure glucose values at pre-injection baseline and 10, 30, 60, 90, and 120 minutes after the injection. **A, C–E, G, and H:** Mice were sacrificed after tail vein sampling, and retinal tissue was analyzed for AMP-activated kinase phosphorylated at Thr 172 (pAMPK) and acetyl CoA carboxylase phosphorylated at Ser 79 (pACC; **A** and **E**), with results quantified in relation to a control protein (**C, D, G, and H**). Data were analyzed by two-way analysis of variance with Bonferroni, Tukey, or Dunnett *post hoc* tests. Data represent means with SEM (**B–D** and **F–H**). \* $P < 0.05$ , \*\* $P < 0.01$ , \*\*\* $P < 0.001$ , and \*\*\*\* $P < 0.0001$ , comparing postinjection time points with the baseline; † $P < 0.05$ , †† $P < 0.01$ , ††† $P < 0.001$ , and †††† $P < 0.0001$ , comparing *db/m* with *db/db* for each time point.

to these patterns in healthy mice, phosphorylation of retinal AMPK and ACC showed no significant changes from baseline in *db/db* mice in response to glucose or insulin boluses at any of the time points interrogated (**Figure 2, C, D, G, and H**).

These results suggest that in healthy mice, signaling through retinal AMPK and ACC is tightly regulated by glucose availability. Strikingly, however, the results in **Figures 1** and **2** show that mice with uncontrolled diabetes lose these regulatory shifts in AMPK and ACC in response to feeding or glucose availability and are hypophosphorylated in relation to healthy controls. Therefore, diabetes is associated with elevated and dysregulated lipogenic signaling in the retina.

#### Light Deprivation and Visual Cycle Inhibition Antagonize Retinal Lipogenic Signals in Diabetes

A prior study showed that genetic ablation of rod photoreceptor lipogenic drive, dependent on the rate-limiting enzyme FAS, reduces the severity of experimental DR.<sup>19</sup>

Following this observation, this study next investigated whether two interventions that impact photoreceptor physiology and effectively reduce DR severity—light deprivation and visual cycle inhibition—converge on AMPK-ACC-FAS lipogenic signaling to influence DR progression.

Oxygen consumption in the mammalian retina increases in dim light conditions. This energetic imbalance likely stems from the need to maintain electrochemical gradients in dark-adapted rods, in which cyclic nucleotide-gated channels are open.<sup>14,39</sup> Light deprivation in early experimental DR prevents the development of later stages of disease.<sup>20</sup> Therefore, the next objective of the present study was to determine whether light deprivation impacts retinal AMPK signaling, via increased ATP use (and, therefore, lower ADP/AMP ratio). Indeed, retinas from healthy, adult mice housed for 2 weeks of 24-hour dark cycles had higher pAMPK levels compared with tissues from control littermates in 12-hour:12-hour light-dark cycles (**Figure 3, A and C**). ACC was also hyper-phosphorylated in dark-adapted retinas compared with light-adapted controls

(Figure 3, A and D). Prolonged dark housing caused approximately 30% reduction in retinal FAS activity (Figure 3E). The effects of light deprivation were specific to retinal tissues because liver levels of pAMPK, pACC, or FAS activity were unaffected by extended dark exposure (Figure 3, B and F–H). These data indicate that light deprivation, presumably by increasing ATP turnover, promotes retinal pAMPK signaling and suppresses pACC-FAS lipogenesis.

Next, dark-induced changes to retinal pAMPK and pACC in diabetes were examined. Under standard lighting conditions, *db/db* mice had hypophosphorylated retinal AMPK and ACC relative to *db/m* controls. However, after 2 weeks of dark housing, *db/db* mice had levels of pAMPK and pACC comparable to light-adapted *db/m* mice (Figure 3, I–K). Similarly, dark-adapted STZ-treated mice had similar levels of retinal pAMPK and pACC as healthy controls, and higher levels than STZ mice in standard lighting (Figure 3, L–N). Consistent with a prior study,<sup>20</sup> dark housing did not change metabolic parameters of the treated mice, including fasting hyperglycemia. Therefore, light deprivation in diabetic mice reversed retinal pAMPK and pACC to levels of healthy controls in standard lighting.

A previous study in mice showed that visual cycle inhibition reduces DR severity.<sup>18</sup> Visual cycle inhibition was associated with reduced retinal reactive oxygen species in that study, but no causative mechanistic relationships were reported.<sup>18</sup> This study therefore tested the hypothesis that pharmacologic visual cycle inhibition prevents DR through similar metabolic signaling mechanisms as prolonged light deprivation. Mice were treated with retinylamine, a potent inhibitor of retinoid isomerohydrolase RPE65 (RPE65). As expected, a 2-week treatment was sufficient to reduce scotopic electroretinographic responses with no observable effects on photopic responses (Figure 4, A–D). Next, retinal pAMPK and pACC levels were measured in mice treated for 2 weeks with retinylamine or a vehicle control. Compared with controls, retinylamine treatment was associated with an approximately 50% increase in pAMPK/actin ratio and an approximately twofold increase in pACC/actin ratio (Figure 4, E–G). These results suggest that retinylamine impedes scotopic visual transduction and, like prolonged dark adaptation, increases AMPK activity and suppresses ACC.

Next, effects of retinylamine on retinal lipogenic signaling in diabetes were assessed. Although retinas from vehicle-treated *db/db* mice had hypophosphorylated AMPK and ACC relative to retinas from healthy *db/m* littermates, 2 weeks of retinylamine treatment in *db/db* mice restored the phosphorylation of both retinal enzymes to control levels (Figure 4, H–J). Likewise, in contrast to that in vehicle-treated STZ mice, retinylamine treatment in STZ-treated diabetic mice restored retinal pAMPK and pACC to control levels (Figure 4, K–M). For the treatment intervals reported in this study, retinylamine did not affect levels of

hyperglycemia in mice with diabetes. Together, these results strongly suggest that visual cycle inhibition in two models of rodent DR reverses diabetes-associated suppression of retinal AMPK and induction of retinal ACC.

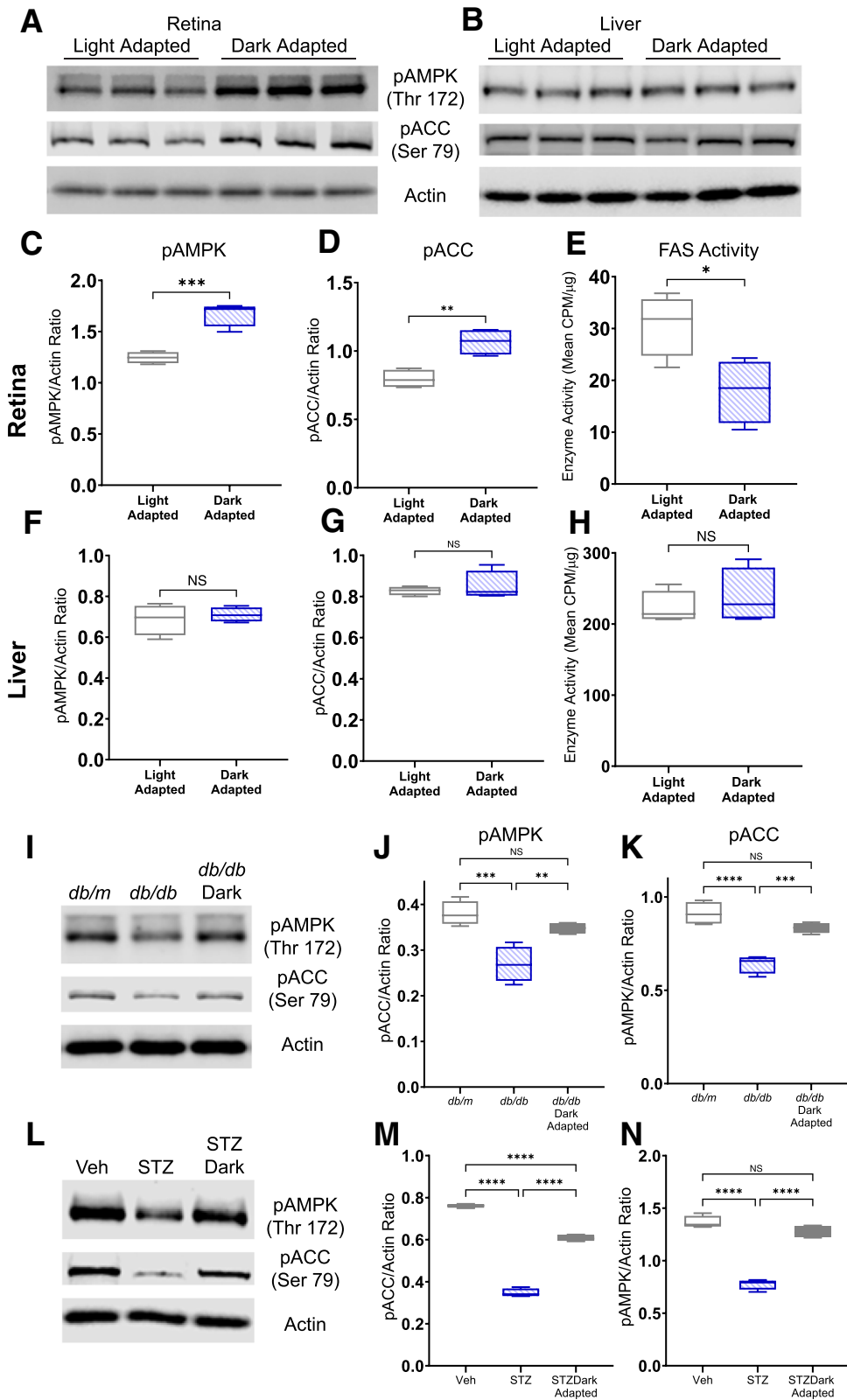
### Protective Effects of Visual Cycle Inhibition in the Diabetic Retina Require Inhibition of Retinal Lipogenesis

Next, whether suppression of ACC-driven lipogenesis is required for the protective effect of retinylamine in DR was examined. Gain-of-function mice expressing FAS R1812W, which show increased susceptibility to DR, were used.<sup>19</sup> Retinal pAMPK and pACC were elevated in mice treated with retinylamine for 2 weeks compared with those given vehicle controls. This increase was detected in both wild-type (WT) and R1812W mice (Figure 5, A–C). In WT mice, retinylamine reduced FAS activity in retinal lysates compared with controls (Figure 5D). In contrast, retinas from R1812W mice showed an approximately 30% increase in FAS retinal enzyme activity over WT controls, which was not reduced by retinylamine (Figure 5D). This indicates that retinylamine exposure is associated with increased retinal AMPK activity, suppressed ACC, but persistently elevated FAS activity in R1812W mice.

Given these results, R1812W mice were used to determine whether retinylamine's effects on DR are dependent on lipogenic signaling. After diabetes induction with STZ for 6 months, WT or R1812W mice were treated twice weekly with i.p. retinylamine for a 3-month regimen. Retinal capillary atrophy was assessed in STZ-treated mice receiving vehicle injections and untreated healthy littermates used as controls (Figure 5, E and F). In WT mice, STZ-induced diabetes mellitus was associated with an approximately twofold increase in atrophic retinal capillaries, whereas STZ-induced diabetes mellitus mice treated with retinylamine showed background levels of capillary atrophy on par with healthy controls (Figure 5G). In contrast, STZ-treated FAS R1812W mice had increases in capillary atrophy over healthy controls that were not prevented by retinylamine exposure (Figure 5H). These results implicate suppression of FAS-regulated lipogenesis as a key protective mechanism of visual cycle inhibition in DR.

## Discussion

Since Arden<sup>7</sup> introduced his alternative hypothesis to early DR pathogenesis >20 years ago, the notion of modulating photoreceptor metabolic activity to treat the disease has been an attractive, yet elusive, goal.<sup>16</sup> In important clinical trials, effects of extended light adaptation on DR were tested using light masks at night to lower rod photoreceptor ATP demand and, by assumption, lessen demand on the retinal vascular supply in diabetes. Yet, in the phase 3 setting, this intervention did not demonstrate efficacy.<sup>17</sup> Similarly,





emixustat—a visual cycle inhibitor acting via blockade of RPE65 isomerase activity—failed to reduce inflammatory cytokine levels in a phase 2 trial of proliferative DR, although it may have reduced macular thickness.<sup>40</sup> On the basis of the results in the present study, an alternative hypothesis may explain both clinical outcomes.

This study confirmed in two different mouse models of DR that retinal lipid metabolic signaling is fundamentally changed by diabetes. Rather than engaging in resting catabolic activities, with those activities increasing during nutrient deprivation and decreasing during nutrient abundance, the diabetic retina is engaged in constitutive anabolic metabolism of lipids. The molecular signature of this signaling is: i) suppressed AMPK (hypophosphorylated); ii) activated ACC (hypophosphorylated); and iii) increased enzymatic activity of FAS. This metabolic network is likely involved in DR pathogenesis because reduction of FAS activity in rods prevents early disease, whereas constitutively active FAS increases susceptibility to it.<sup>19</sup>

The findings of the present study are best applied to DR when its pathogenesis is modeled into at least two distinct phases, beyond classic vascular staging systems.<sup>41,42</sup> The latter phase is characterized by visible microvasculopathy, where tissue ischemia and vascular endothelial growth factor secretion are driving factors. However, prodromal, an early phase, is characterized by dysmetabolism of photoreceptors, which engage in excess lipid synthetic activity driven by systemic hyperglycemia and unchecked intraretinal transport of glucose via non—insulin-dependent glucose transporter type 1 (GLUT1) and glucose transporter type 3 (GLUT3).<sup>43</sup> The results of this study suggest that dark adaptation provides a physiological outlet for excess ATP in the diabetic retina and reversal of the anabolic drive. Indeed, phosphorylation states of retinal AMPK and ACC in light-deprived diabetic mice were comparable to those of healthy light-adapted controls (Figure 3, I–N). Furthermore, prolonged dark adaptation does not exacerbate tissue ischemia in prodromal DR, because vascular endothelial growth factor levels are normal and nonperfusion is absent or negligible during this phase.<sup>20</sup>

Operating in a similar manner, visual cycle inhibition with retinylamine decreased retinal anabolic activity, as characterized by hyper-phosphorylated AMPK and ACC (Figure 4). More importantly, retinylamine treatment did not prevent

diabetes-induced retinal capillary damage in FAS R1812W mice with constitutively active FAS, strongly suggesting that visual cycle inhibition works to alleviate prodromal DR by increasing energetic demands and inhibiting lipid anabolic activity (Figure 5). Findings from a study using manganese-enhanced magnetic resonance imaging and the RPE65 inhibitor emixustat suggest that visual cycle inhibition lowers the metabolic demand of dark activity in the retina, rather than increasing it, as observed in the current study.<sup>44</sup> The discrepancy may be due to differences in assessing metabolic demand: this study used an endogenous cellular metabolic sensor—AMPK—to gauge metabolic demand, whereas they used cation flux imaging; and distinct effects of retinylamine compared with emixustat on RPE65 inhibition.

The effects observed in the present study with prolonged dark adaptation and visual cycle inhibition on AMPK-dependent cellular signaling in the retina are akin to the molecular effects of aerobic exercise on skeletal muscle. In response to exercise, muscle ATP consumption is increased by >100-fold, leading to an increase in intracellular AMP and an activation of AMPK in a time- and intensity-dependent manner.<sup>45,46</sup> AMPK signaling up-regulates cellular pathways that produce ATP (catabolic pathways) and inhibits those that store ATP for later use (anabolic pathways). Similarly, in healthy and diabetic retina, prolonged dark adaptation and visual cycle inhibition both cause activation of retinal AMPK, presumably by increasing ATP turnover stemming from sustained activity of the dark current in photoreceptors. This study also showed that activation of AMPK by retinylamine reduced DR severity, but that this protective effect was abolished in the presence of constitutively active lipid anabolism (FAS R1812W).

The results of this study suggest that ACC-FAS axis is a crucial early driver of prodromal DR. On the basis of prior studies using targeted genetic disruptions of FAS,<sup>19</sup> it is likely that aberrant signaling of rod photoreceptors is most important for DR pathogenesis. How photoreceptor pathology might impact retinal capillary health in diabetes remains unclear. Among several explanations, some possibilities include changes to regional blood flow patterns due to photoreceptor dysmetabolism and subsequent tissue hypoxia, impairment of neurovascular coupling mechanisms, leading to direct vascular injury, or increases in outer retinal oxidative stress and resulting inflammatory responses

**Figure 3** Effects of prolonged dark adaptation on retinal cellular nutrient sensors and retinal *de novo* lipogenesis. The 3-month-old C57BL/6J littermate mice were randomized to housing with normal 12-hour:12-hour light-dark cycle or to 24-hour dark cycles. After 2 weeks, retinal and liver tissues were harvested and analyzed. **A–H:** Representative Western blot analyses for AMP-activated kinase phosphorylated at Thr 172 (pAMPK) and acetyl CoA carboxylase phosphorylated at Ser 79 (pACC) are shown for retina (**A**) and liver (**B**), with quantification of values, normalized to  $\beta$ -actin (**C**, **D**, **F**, and **G**). In a subgroup of mice, retinal (**E**) and liver (**H**) tissue was harvested and analyzed for fatty acid synthase (FAS) activity, normalized to total protein content. Data were analyzed by *t*-tests. **I–N:** The 6-month-old *db/db* mice (**I–K**) or streptozotocin (STZ)-treated mice (**L–N**) were randomized to 2 weeks of 12-hour:12-hour light-dark cycle housing or to 24-hour dark housing, and were analyzed for retinal pAMPK and pACC levels, compared with nondiabetic controls in normal light-dark cycles (either *db/m* for *db/db* mice; or vehicle (Veh)-treated littermates for STZ-treated mice). **J**, **K**, **M**, and **N:** Levels of pAMPK or pACC, normalized to  $\beta$ -actin, were compared across subgroups in each diabetes model. Data were analyzed by one-way analysis of variance with Tukey *post hoc* tests. Data represent means with interquartile ranges (**C–H**, **J**, **K**, **M**, and **N**). \**P* < 0.05, \*\**P* < 0.01, \*\*\**P* < 0.001, and \*\*\*\**P* < 0.0001. NS, not statistically significant.

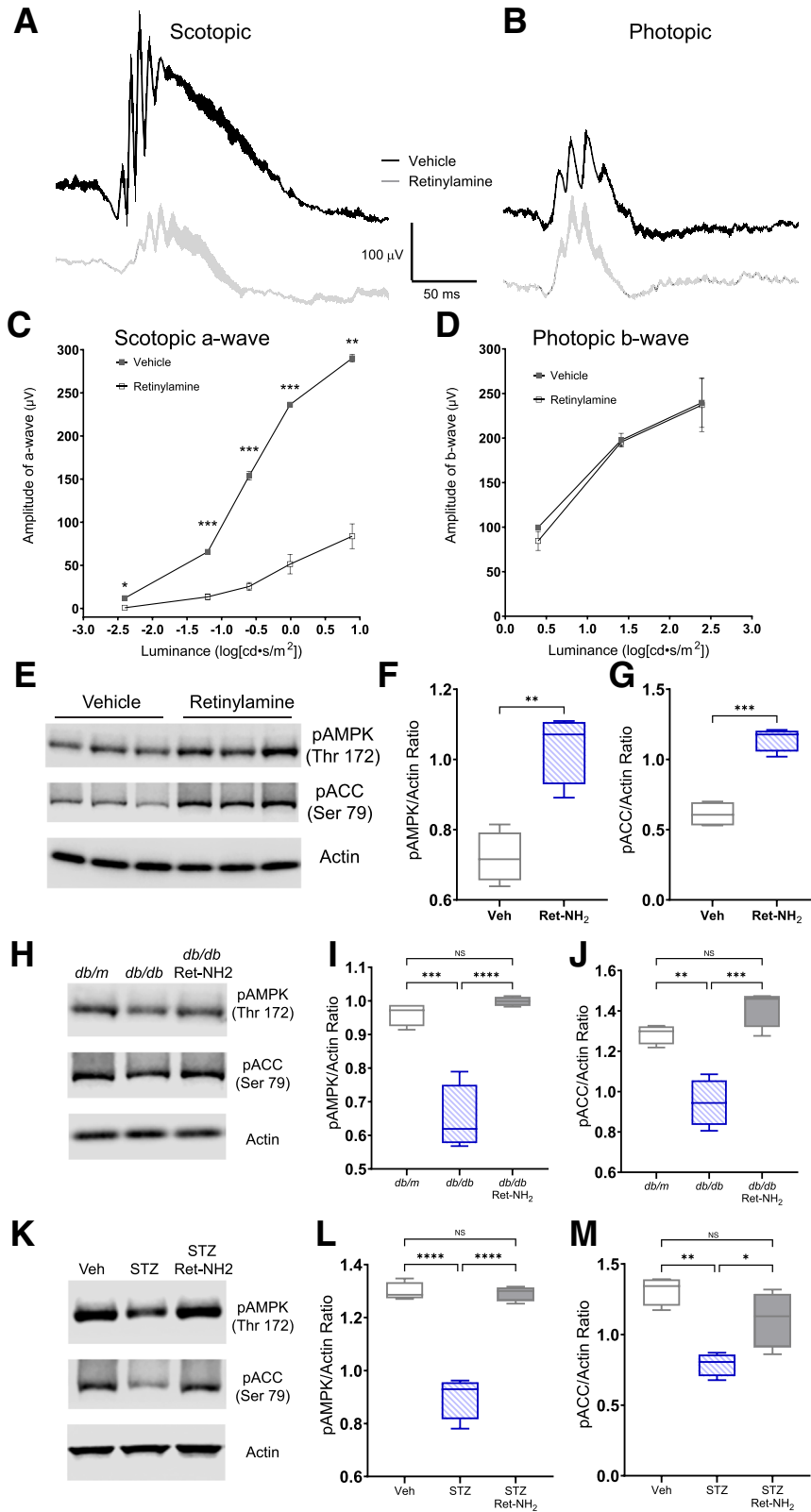


**Figure 4** Effects of visual cycle inhibition on retinal cellular nutrient sensors and retinal *de novo* lipogenesis. The 3-month-old C57BL/6J littermate mice were randomized to treatment with retinylamine (Ret-NH<sub>2</sub>) or vehicle, twice weekly by i.p. injection for 2 weeks. Full-field electroretinography was performed to assess effects of the drug. **A–D**: Scotopic responses to a  $-1.20 \log(\text{cd}\cdot\text{s}/\text{m}^2)$  luminance white flash (**A**) and photopic responses to a  $1.41 \log(\text{cd}\cdot\text{s}/\text{m}^2)$  luminance white flash (**B**) are shown, with quantification of luminance-response curves of the scotopic a-waves (**C**) and photopic b-waves (**D**). Data were analyzed by two-way analysis of variance with Bonferroni *post hoc* tests. In the same mice, retinal tissue was then harvested and analyzed for AMP-activated kinase phosphorylated at Thr 172 (pAMPK) and acetyl CoA carboxylase phosphorylated at Ser 79 (pACC). **E–G**: Representative blots (**E**) with quantification of values, normalized to  $\beta$ -actin (**F** and **G**), are shown. Data were analyzed by *t*-tests. **H–M**: The 6-month-old *db/db* mice (**H–J**) or streptozotocin (STZ)-treated mice (**K–M**) were randomized to 2 weeks of twice-weekly Ret-NH<sub>2</sub> or vehicle treatment, and were analyzed for retinal pAMPK and pACC levels, compared with vehicle-treated nondiabetic controls (either *db/m* for *db/db* mice; or citrate buffer-treated littermates for STZ-treated mice). **I**, **J**, **L**, and **M**: Levels of pAMPK or pACC, normalized to  $\beta$ -actin, were compared across subgroups in each diabetes model. Data were analyzed by one-way analysis of variance with Tukey *post hoc* tests. Data represent means with SEM (**C** and **D**) or means with interquartile ranges (**F**, **G**, **I**, **J**, **L**, and **M**). \* $P < 0.05$ , \*\* $P < 0.01$ , \*\*\* $P < 0.001$ , and \*\*\*\* $P < 0.0001$ . NS, not statistically significant.

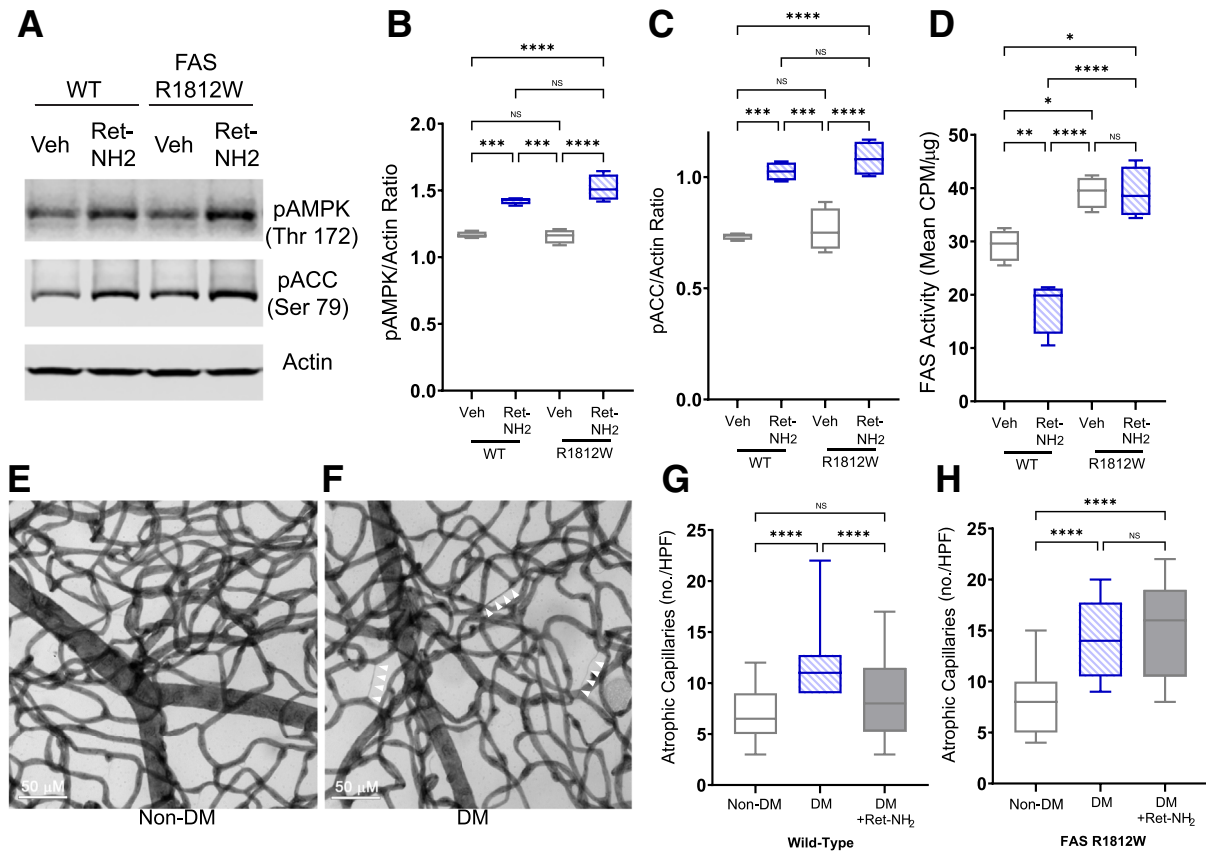


**Figure 5** Prevention of diabetic retinopathy by visual cycle inhibition in streptozotocin (STZ)-treated mice is dependent on inhibition of *de novo* lipogenesis. The 3-month-old FASR18W transgenic mice or wild-type (WT) littermate control mice were randomized to treatment with retinylamine (Ret-NH<sub>2</sub>) or vehicle (Veh), twice weekly by i.p. injection for 2 weeks. Retinal tissue was then harvested from all mice and analyzed for AMP-activated kinase phosphorylated at Thr 172 (pAMPK) and acetyl CoA carboxylase phosphorylated at Ser 79 (pACC). **A–C:** Representative blots (**A**) with quantification of values, normalized to  $\beta$ -actin (**B** and **C**), are shown. **D:** In a subgroup of mice, retinal tissue was harvested and analyzed for fatty acid synthase (FAS) activity, normalized to total protein content. Data were analyzed by one-way analysis of variance with Tukey *post hoc* tests. In a separate cohort, 6-month-old STZ-treated mice (in either wild-type FAS or FAS R1812W genetic backgrounds) were treated with Ret-NH<sub>2</sub> or vehicle twice weekly for 3 months. **E** and **F:** Capillaries were then assessed in retinal trypsin digest preparations (**E**) with quantification of thin-atrophic capillaries (arrowheads; **F**). **G** and **H:** The number of atrophic capillaries per field was compared across groups, including vehicle-injected nondiabetic controls. Data were analyzed by one-way analysis of variance with Tukey *post hoc* tests. Data represent means with interquartile ranges (**B–D**, **G**, and **H**). \**P* < 0.05, \*\**P* < 0.01, \*\*\**P* < 0.001, and \*\*\*\**P* < 0.0001. Scale bars = 50  $\mu$ m (**E** and **F**). DM, diabetes mellitus; HPF, high-power field; NS, not statistically significant.

that damage vessels. It is also possible that combinations of some or all of these mechanisms are causative.

Pharmacotherapy directed at correcting early metabolic abnormalities in rods could represent a novel DR intervention at the prodromal stage, entirely independent of the vascular endothelial growth factor-centric treatments that are effective in manifest DR. Although the present study assayed retinal capillary health as an end point of DR, interventions were provided at much earlier stages, when tissue hypoxia was not present. The results of this study suggest that emixustat given at earlier stages than previously studied, such as non-proliferative DR before Early Treatment Diabetic Retinopathy Study level 47 or even earlier (before the development of cascading ischemia), would be more likely to produce a clinically meaningful response. Moreover, emixustat would not be expected to show benefits in proliferative DR, a condition with widespread retinal nonperfusion and ischemia.

The results of this study also suggest that non-pharmaceutical therapy could also be an important adjunct to management of prodromal DR. Specifically, this study showed that prolonged dark adaptation increased retinal AMPK signaling and prevented late-stage DR.<sup>20</sup> Although the paradigm for light deprivation used here is neither practical nor ethical in humans, perhaps improved artificial light hygiene in patients with diabetes could be useful in mitigating the onset of manifest DR. Indeed, the effects of light pollution in modern lifestyles (ie, the prolongation of the photoperiod, especially with the increasing use of bright portable screens) on disruption of circadian biology are well established.<sup>47</sup> Although correcting those circadian abnormalities themselves is hypothesized to have beneficial metabolic effects in diabetes,<sup>48</sup> retinal health could be improved by mechanisms largely independent of circadian biology, specifically those mediated by reduction in photoreceptor anabolic metabolism.

## Author Contributions

S.Z. and R.R. performed experiments and wrote the manuscript; X.W. performed experiments, contributed to discussions, and edited the manuscript; M.B. and S.J. edited the manuscript; and M.G. and C.F.S. contributed to discussions and edited manuscript.

## Disclosure Statement

None declared.

## References

- Antonetti DA: The neuroscience of diabetic retinopathy. *Vis Neurosci* 2021, 38:E001
- Antonetti DA, Silva PS, Stitt AW: Current understanding of the molecular and cellular pathology of diabetic retinopathy. *Nat Rev Endocrinol* 2021, 17:195–206
- Tonade D, Kern TS: Photoreceptor cells and RPE contribute to the development of diabetic retinopathy. *Prog Retin Eye Res* 2021, 83:100919
- McAnany JJ, Park JC: Temporal frequency abnormalities in early-stage diabetic retinopathy assessed by electroretinography. *Invest Ophthalmol Vis Sci* 2018, 59:4871–4879
- McAnany JJ, Park JC: Cone photoreceptor dysfunction in early-stage diabetic retinopathy: association between the activation phase of cone phototransduction and the Flicker electroretinogram. *Invest Ophthalmol Vis Sci* 2019, 60:64–72
- McAnany JJ, Park JC: Rod photoreceptor activation and deactivation in early-stage diabetic eye disease. *Doc Ophthalmol* 2023, 146:229–239
- Arden GB: The absence of diabetic retinopathy in patients with retinitis pigmentosa: implications for pathophysiology and possible treatment. *Br J Ophthalmol* 2001, 85:366–370
- Chen YF, Chen HY, Lin CC, Chen MS, Chen PC, Wang IJ: Retinitis pigmentosa reduces the risk of proliferative diabetic retinopathy: a nationwide population-based cohort study. *PLoS One* 2012, 7:e45189
- Sternberg P Jr, Landers MB 3rd, Wolbarsht M: The negative coincidence of retinitis pigmentosa and proliferative diabetic retinopathy. *Am J Ophthalmol* 1984, 97:788–789
- Yokomizo H, Maeda Y, Park K, Clermont AC, Hernandez SL, Fickweiler W, Li Q, Wang CH, Paniagua SM, Simao F, Ishikado A, Sun B, Wu IH, Katagiri S, Poher DM, Tinsley LJ, Avery RL, Feener EP, Kern TS, Keenan HA, Aiello LP, Sun JK, King GL: Retinol binding protein 3 is increased in the retina of patients with diabetes resistant to diabetic retinopathy. *Sci Transl Med* 2019, 11:eaa06627
- Liu H, Tang J, Du Y, Saadane A, Samuels I, Veenstra A, Kiser JZ, Palczewski K, Kern TS: Transducin1, phototransduction and the development of early diabetic retinopathy. *Invest Ophthalmol Vis Sci* 2019, 60:1538–1546
- Berkowitz BA, Grady EM, Khetarpal N, Patel A, Roberts R: Oxidative stress and light-evoked responses of the posterior segment in a mouse model of diabetic retinopathy. *Invest Ophthalmol Vis Sci* 2015, 56:606–615
- Du Y, Veenstra A, Palczewski K, Kern TS: Photoreceptor cells are major contributors to diabetes-induced oxidative stress and local inflammation in the retina. *Proc Natl Acad Sci U S A* 2013, 110:16586–16591
- Okawa H, Sampath AP, Laughlin SB, Fain GL: ATP consumption by mammalian rod photoreceptors in darkness and in light. *Curr Biol* 2008, 18:1917–1921
- Arshavsky VY, Burns ME: Photoreceptor signaling: supporting vision across a wide range of light intensities. *J Biol Chem* 2012, 287:1620–1626
- Arden GB, Sidman RL, Arap W, Schlingemann RO: Spare the rod and spoil the eye. *Br J Ophthalmol* 2005, 89:764–769
- Sivaprasad S, Vasconcelos JC, Prevost AT, Holmes H, Hykin P, George S, Murphy C, Kelly J, Arden GB; CLEOPATRA Study Group: Clinical efficacy and safety of a light mask for prevention of dark adaptation in treating and preventing progression of early diabetic macular oedema at 24 months (CLEOPATRA): a multicentre, phase 3, randomised controlled trial. *Lancet Diabetes Endocrinol* 2018, 6:382–391
- Liu H, Tang J, Du Y, Lee CA, Golczak M, Muthusamy A, Antonetti DA, Veenstra AA, Amengual J, von Lintig J, Palczewski K, Kern TS: Retinylamine benefits early diabetic retinopathy in mice. *J Biol Chem* 2015, 290:21568–21579
- Rajagopal R, Sylvester B, Zhang S, Adak S, Wei X, Bowers M, Jessberger S, Hsu FF, Semenkovich CF: Glucose-mediated de novo lipogenesis in photoreceptors drives early diabetic retinopathy. *J Biol Chem* 2021, 297:101104
- Thebeau C, Zhang S, Kolesnikov AV, Kefalov VJ, Semenkovich CF, Rajagopal R: Light deprivation reduces the severity of experimental diabetic retinopathy. *Neurobiol Dis* 2020, 137:104754
- Bowers M, Liang T, Gonzalez-Bohorquez D, Zocher S, Jaeger BN, Kovacs WJ, Rohrl C, Cramb KML, Winterer J, Kruse M, Dimitrieva S, Overall RW, Wegleiter T, Najmabadi H, Semenkovich CF, Kempermann G, Foldy C, Jessberger S: FASN-dependent lipid metabolism links neurogenic stem/progenitor cell activity to learning and memory deficits. *Cell Stem Cell* 2020, 27:98–109.e11
- Feit-Leichman RA, Kinouchi R, Takeda M, Fan Z, Mohr S, Kern TS, Chen DF: Vascular damage in a mouse model of diabetic retinopathy: relation to neuronal and glial changes. *Invest Ophthalmol Vis Sci* 2005, 46:4281–4287
- Saadane A, Lessieur EM, Du Y, Liu H, Kern TS: Successful induction of diabetes in mice demonstrates no gender difference in development of early diabetic retinopathy. *PLoS One* 2020, 15:e0238727
- Geisler CE, Hepler C, Higgins MR, Renquist BJ: Hepatic adaptations to maintain metabolic homeostasis in response to fasting and refeeding in mice. *Nutr Metab* 2016, 13:62
- Towers AE, Oelschlager ML, Juda MB, Jain S, Gainey SJ, Freund GG: HFD refeeding in mice after fasting impairs learning by activating caspase-1 in the brain. *Metab Clin Exp* 2020, 102:153989
- Rajagopal R, Zhang S, Wei X, Doggett T, Adak S, Enright J, Shah V, Ling G, Chen S, Yoshino J, Hsu FF, Semenkovich CF: Retinal de novo lipogenesis coordinates neurotrophic signaling to maintain vision. *JCI Insight* 2018, 3:14
- Golczak M, Kuksa V, Maeda T, Moise AR, Palczewski K: Positively charged retinoids are potent and selective inhibitors of the trans-cis isomerization in the retinoid (visual) cycle. *Proc Natl Acad Sci U S A* 2005, 102:8162–8167
- Rajagopal R, Bligard GW, Zhang S, Yin L, Lukasiewicz P, Semenkovich CF: Functional deficits precede structural lesions in mice with high-fat diet-induced diabetic retinopathy. *Diabetes* 2016, 65:1072–1084
- Robison WG Jr, McCaleb ML, Feld LG, Michaelis OE, Laver N, Mercandetti M: Degenerated intramural pericytes (“ghost cells”) in the retinal capillaries of diabetic rats. *Curr Eye Res* 1991, 10:339–350
- Veenstra A, Liu H, Lee CA, Du Y, Tang J, Kern TS: Diabetic retinopathy: retina-specific methods for maintenance of diabetic rodents and evaluation of vascular histopathology and molecular abnormalities. *Curr Protoc Mol Biol* 2015, 5:247–270
- Lin SC, Hardie DG: AMPK: sensing glucose as well as cellular energy status. *Cell Metab* 2018, 27:299–313
- Suter M, Riek U, Tuerk R, Schlattner U, Wallimann T, Neumann D: Dissecting the role of 5'-AMP for allosteric stimulation, activation,

- and deactivation of AMP-activated protein kinase. *J Biol Chem* 2006, 281:32207–32216
33. Hawley SA, Pan DA, Mustard KJ, Ross L, Bain J, Edelman AM, Frenguelli BG, Hardie DG: Calmodulin-dependent protein kinase kinase-beta is an alternative upstream kinase for AMP-activated protein kinase. *Cell Metab* 2005, 2:9–19
  34. Woods A, Johnstone SR, Dickerson K, Leiper FC, Fryer LG, Neumann D, Schlattner U, Wallimann T, Carlson M, Carling D: LKB1 is the upstream kinase in the AMP-activated protein kinase cascade. *Curr Biol* 2003, 13:2004–2008
  35. Wakil SJ, Abu-Elheiga LA: Fatty acid metabolism: target for metabolic syndrome. *J Lipid Res* 2009, 50 Suppl:S138–S143
  36. Semenkovich CF: Regulation of fatty acid synthase (FAS). *Prog Lipid Res* 1997, 36:43–53
  37. Ha J, Daniel S, Broyles SS, Kim KH: Critical phosphorylation sites for acetyl-CoA carboxylase activity. *J Biol Chem* 1994, 269:22162–22168
  38. Hunkeler M, Hagmann A, Stutfeld E, Chami M, Guri Y, Stahlberg H, Maier T: Structural basis for regulation of human acetyl-CoA carboxylase. *Nature* 2018, 558:470–474
  39. Linsenmeier RA: Effects of light and darkness on oxygen distribution and consumption in the cat retina. *J Gen Physiol* 1986, 88:521–542
  40. Kubota R, Jhaveri C, Koester JM, Gregory JK: Effects of emixustat hydrochloride in patients with proliferative diabetic retinopathy: a randomized, placebo-controlled phase 2 study. *Graefes Arch Clin Exp Ophthalmol* 2021, 259:369–378
  41. Saadane A, Du Y, Thoreson WB, Miyagi M, Lessieur EM, Kiser J, Wen X, Berkowitz BA, Kern TS: Photoreceptor cell calcium dysregulation and calpain activation promote pathogenic photoreceptor oxidative stress and inflammation in prodromal diabetic retinopathy. *Am J Pathol* 2021, 191:1805–1821
  42. Sun JK, Aiello LP, Abramoff MD, Antonetti DA, Dutta S, Pragnell M, Levine SR, Gardner TW: Updating the staging system for diabetic retinal disease. *Ophthalmology* 2021, 128:490–493
  43. Mantych GJ, Hageman GS, Devaskar SU: Characterization of glucose transporter isoforms in the adult and developing human eye. *Endocrinology* 1993, 133:600–607
  44. Kubota R, Calkins DJ, Henry SH, Linsenmeier RA: Emixustat reduces metabolic demand of dark activity in the retina. *Invest Ophthalmol Vis Sci* 2019, 60:4924–4930
  45. Gaitanos GC, Williams C, Boobis LH, Brooks S: Human muscle metabolism during intermittent maximal exercise. *J Appl Physiol* 1993, 75:712–719
  46. Wojtaszewski JF, Nielsen P, Hansen BF, Richter EA, Kiens B: Isoform-specific and exercise intensity-dependent activation of 5'-AMP-activated protein kinase in human skeletal muscle. *J Physiol* 2000, 528:221–226
  47. Huang W, Ramsey KM, Marcheva B, Bass J: Circadian rhythms, sleep, and metabolism. *J Clin Invest* 2011, 121:2133–2141
  48. Mason IC, Qian J, Adler GK, Scheer F: Impact of circadian disruption on glucose metabolism: implications for type 2 diabetes. *Diabetologia* 2020, 63:462–472